

Spatial coherence effects on second- and fourth-order temporal interference

Timothy Yarnall^{1,2}, Ayman F. Abouraddy³, Bahaa E. A. Saleh², and Malvin C. Teich²

¹ *Lincoln Laboratory, Massachusetts Institute of Technology, 244 Wood Street, Lexington, Massachusetts, 02420-9108, USA*

² *Quantum Imaging Laboratory, Departments of Electrical & Computer Engineering and Physics, Boston University, Boston, Massachusetts 02215-2421, USA*

³ *Research Laboratory of Electronics, Massachusetts Institute of Technology, Cambridge, Massachusetts 02139-4307, USA*

Abstract: We report the results of two experiments performed with two-photon light, produced via collinear degenerate optical spontaneous parametric downconversion (SPDC), in which both second-order (one-photon) and fourth-order (two-photon) interferograms are recorded in a Mach–Zehnder interferometer (MZI). In the first experiment, high-visibility fringes are obtained for both the second- and fourth-order interferograms. In the second experiment, the MZI is modified by the removal of a mirror from one of its arms; this leaves the fourth-order interferogram unchanged, but extinguishes the second-order interferogram. A theoretical model that takes into consideration both the temporal and spatial degrees-of-freedom of the two-photon state successfully explains the results. While the temporal interference in the MZI is independent of the spatial coherence of the source, that of the modified MZI is not.

© 2008 Optical Society of America

OCIS codes: (270.1670) Coherent optical effects; (120.3180) Interferometry; (270.5585) Quantum information and processing

References and links

1. M. A. Horne, A. Shimony, and A. Zeilinger, “Two-particle interferometry,” *Phys. Rev. Lett.* **62**, 2209–2212 (1989).
2. D. M. Greenberger, M. A. Horne, and A. Zeilinger, “Multiparticle Interferometry and the Superposition Principle,” *Phys. Today* **8**(46), 22–29 (1993).
3. M. Horne, A. Shimony, and A. Zeilinger, “Two-particle interferometry,” *Nature (London)* **347**, 429–430 (1990).
4. G. Jaeger, M. A. Horne, and A. Shimony, “Complementarity of one-particle and two-particle interference,” *Phys. Rev. A* **48**, 1023–1027 (1993).
5. G. Jaeger, A. Shimony, and L. Vaidman, “Two interferometric complementarities,” *Phys. Rev. A* **51**, 54–67 (1995).
6. C. K. Hong, Z. Y. Ou, and L. Mandel, “Measurement of Subpicosecond Time Intervals between Two Photons by Interference,” *Phys. Rev. Lett.* **59**, 2044–2046 (1987).
7. S. P. Walborn, A. N. de Oliveira, S. Pádua, and C. H. Monken, “Multimode Hong–Ou–Mandel Interference,” *Phys. Rev. Lett.* **90**, 143601 (2003).
8. T. S. Larchuk, R. A. Campos, J. G. Rarity, P. R. Tapster, E. Jakeman, B. E. A. Saleh, and M. C. Teich, “Interfering entangled photons of different colors,” *Phys. Rev. Lett.* **70**, 1603–1606 (1993).
9. J. D. Franson, “Two-photon interferometry over large distances,” *Phys. Rev. A* **44**, 4552–4555 (1991).
10. J. G. Rarity and P. R. Tapster, “Fourth-order interference effects at large distances,” *Phys. Rev. A* **45**, 2052–2056 (1992).
11. D. V. Strekalov, T. B. Pittman, A. V. Sergienko, Y. H. Shih, and P. G. Kwiat, “Postselection-free energy-time entanglement,” *Phys. Rev. A* **54**, R1–R4 (1996).

12. J. G. Rarity, P. R. Tapster, E. Jakeman, T. Larchuk, R. A. Campos, M. C. Teich, and B. E. A. Saleh, "Two-Photon Interference in a Mach-Zehnder Interferometer," *Phys. Rev. Lett.* **65**, 1348–1351 (1990).
 13. A. F. Abouraddy, M. B. Nasr, B. E. A. Saleh, A. V. Sergienko, and M. C. Teich, "Demonstration of the complementarity of one- and two-photon interference," *Phys. Rev. A* **63**, 063803 (2001).
 14. C. Santori, D. Fattal, J. Vuckovic, G. S. Solomon, and Y. Yamamoto, "Indistinguishable photons from a single-photon device," *Nature (London)* **419**, 594–597 (2002).
 15. H. Sasada and M. Okamoto, "Transverse-mode beam splitter of a light beam and its application to quantum cryptography," *Phys. Rev. A* **68**, 012323 (2003).
 16. A. F. Abouraddy, T. Yarnall, B. E. A. Saleh, and M. C. Teich, "Violation of Bells inequality with continuous spatial variables," *Phys. Rev. A* **75**, 052114 (2007).
 17. T. Yarnall, A. F. Abouraddy, B. E. A. Saleh, and M. C. Teich, "Synthesis and Analysis of Entangled Photonic Qubits in Spatial-Parity Space," *Phys. Rev. Lett.* **99**, 250502 (2007).
 18. M. Segev, R. Solomon, and A. Yariv, "Manifestation of Berry's phase in image-bearing optical beams," *Phys. Rev. Lett.* **69**, 590–592 (1992).
 19. M. P. van Exter, P. S. K. Lee, S. Doesburg, and J. P. Woerdman, "Mode counting in high-dimensional orbital angular momentum entanglement," *Opt. Express* **15**, 6431–6438 (2007), URL <http://www.opticsexpress.org/abstract.cfm?URI=oe-15-10-6431>.
 20. S. E. Harris, M. K. Oshman, and R. L. Byer, "Observation of tunable optical parametric fluorescence," *Phys. Rev. Lett.* **18**, 732–735 (1967).
 21. A. Zeilinger, "Quantum entanglement: A fundamental concept finding its applications," *Physica Scripta* **T76**, 203–209 (1998).
 22. J. T. Barreiro, N. K. Langford, N. A. Peters, and P. G. Kwiat, "Generation of Hyperentangled Photon Pairs," *Phys. Rev. Lett.* **95**, 260501 (2005).
 23. B. E. A. Saleh, A. F. Abouraddy, A. V. Sergienko, and M. C. Teich, "Duality between partial coherence and partial entanglement," *Phys. Rev. A* **62**, 043816 (2000).
-

1. Introduction

Two-photon interference experiments reflect correlations that are fourth-order in the optical field and second-order in the intensity, while one-photon interference experiments reflect correlations that are second-order in the field and first-order in the intensity. It is sometimes taken as a rule-of-thumb in quantum optics that two-photon interference experiments displaying high two-photon visibility V_{12} must necessarily display low one-photon visibility V_1 [1]. We examine this issue experimentally by carrying out two-photon (coincidence) measurements using a pair of detectors to determine the correlation function $G^{(2)}(\tau)$ and, simultaneously, one-photon (singles) measurements using a single detector to determine the intensity $I(\tau)$, for the same optical field.

We demonstrate in this paper that this rule-of-thumb can be rigorously supported only when each photon of the two-photon state is sent into a separate two-path interferometer that acts on a single physical degree of freedom (and may thus be represented by an $SU(2)$ transformation) [2, 3]. The visibilities for a two-photon state in such a configuration are indeed complementary such that they satisfy $V_{12}^2 + V_1^2 \leq 1$, where the equality holds for pure two-photon states [4, 5]. This complementarity is not applicable, however, when both photons are directed into the *same* interferometer, nor does it apply when more than one degree-of-freedom is probed by the interferometer. The most notable counterexamples of this rule-of-thumb in temporal interferometry can be found in the interferograms recorded with Hong–Ou–Mandel (HOM) [6] and Mach–Zehnder interferometers (MZI).

At first blush, experiments performed using a HOM interferometer in conjunction with the two-photon state produced by spontaneous parametric downconversion (SPDC) appear to confirm the rule-of-thumb: when the temporal delay is scanned, high-visibility two-photon interference (the HOM dip) is observed and $V_{12} = 1$, while the singles rate remains flat at $V_1 = 0$ [6]. It has recently been shown however, that by manipulating the *spatial* distribution of the pump, the visibility of the temporal HOM dip may be varied from unity to zero, while the singles rate remains unchanged (i.e., exhibiting no interference) [7]. Moreover, it has been shown experimentally that the rule-of-thumb does not hold for an MZI in which each photon of a two-photon

SPDC state was directed to a different input port of the same MZI; high V_1 and V_{12} have been simultaneously observed [8].

Clearly, complementarity in the visibilities of one- and two-photon interference is not universally applicable. Other examples of two-photon interferometry that make use of two-photon sources, in which each photon is sent into a different interferometer, include the experiments reported in Refs. [9, 10, 11]. Examples in which both photons are sent into the same interferometer include the experiments reported in Refs. [12, 13, 14].

In this paper, we consider a slightly different question: can the visibility of second-order interference be changed without affecting the fourth-order interference? To address this issue, we examine the two-photon interference in a MZI from a fresh perspective and show that, surprisingly, *high or low second-order* interference ($V_1 = 1$ or $V_1 = 0$) may be observed while retaining *high fourth-order* interference ($V_{12} = 1$). This effect is the opposite of that reported by Walborn *et al.* [7]; moreover, in our case, the change in the second-order interference visibility is achieved *without* altering the spatial distribution of the source. Our results thus demonstrate both a confirmation of, and a departure from, the rule-of-thumb in two closely related, but distinct, experimental configurations.

2. Experiment

The experimental configurations under discussion differ only in the form of the Mach-Zehnder interferometer. As depicted in Fig. 1, the first is a traditional MZI in which the delay τ between the interfering paths is varied. The second is a MZI in which a spatial flip (SF) has been inserted into one arm of the interferometer [15, 16, 17]; we refer to this as a modified Mach-Zehnder interferometer (MZIM). The spatial flip is achieved by unbalancing the number of mirrors in the two interferometer arms; since the flip is carried out only in one spatial dimension, it is readily implemented by simply removing or adding a single mirror. No use is made of out-of-plane reflections, such as those reported in Refs. [18, 19]. In both cases, the input light is in a two-photon state produced via SPDC [20], with both entangled photons entering the same input port of the interferometer.

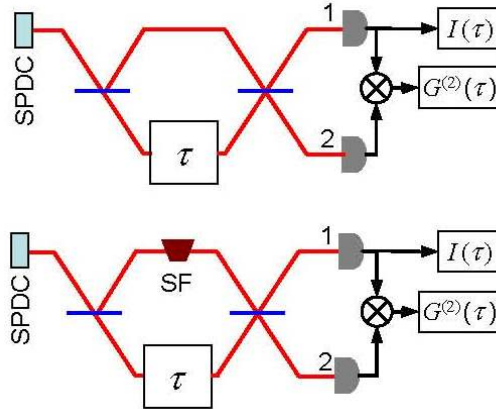


Fig. 1. Conceptual layout for two Mach-Zehnder interferometer experiments. The upper diagram illustrates the traditional MZI while the lower diagram illustrates a modified version (MZIM) in which a spatial flip (SF) has been inserted into one arm. Both are followed by detectors that record the coincidence rate at the two output ports, $G^{(2)}(\tau)$, as well as the singles rate, $I(\tau)$.

The setups for the MZI and MZIM experiments are shown in more detail in Fig. 2(a). A linearly polarized monochromatic pump laser diode (wavelength 405 nm, power 50 mW) illuminates a 1.5-mm-thick β -barium borate (BBO) nonlinear optical crystal (NLC) in a collinear type-I configuration (signal and idler photons have the same polarization, orthogonal to that of the pump). The pump is removed by using a polarizing beam splitter placed after the crystal as well as by interference filters (centered at 810 nm, 10-nm bandwidth) placed in front of the detectors D_1 and D_2 (EG&G SPCM-AQR-15-FC), the outputs of which are fed to a coincidence circuit (denoted \otimes) and thence to a counter. The bandwidth of the interference filters is smaller than that of the SPDC-generated two-photon state, so that the widths of temporal interference features, such as the HOM dip and the MZI interferogram, are expected to be proportional to the inverse of the filter bandwidth.

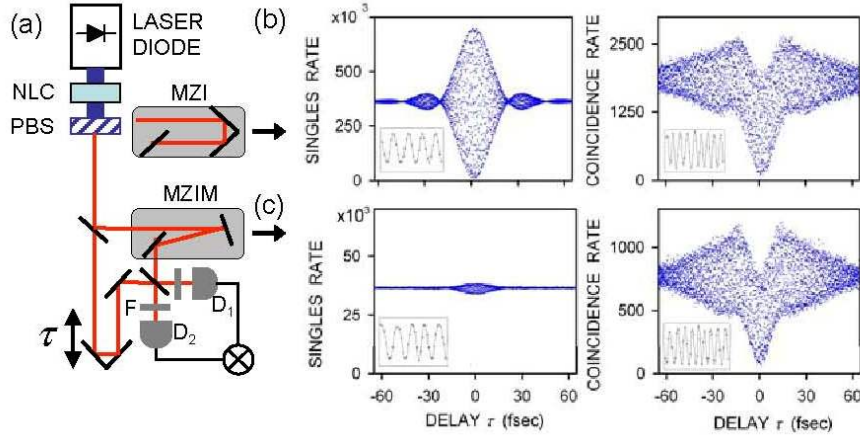


Fig. 2. (a) Schematic of the Mach-Zehnder experimental arrangements for studying second- and fourth-order temporal interference. NLC: nonlinear crystal; PBS: polarizing beam splitter; F: interference filter; D: detector; \otimes : coincidence circuit. The upper shaded region highlights one arm of the traditional Mach-Zehnder interferometer (MZI), which comprises three mirrors, while the lower shaded region highlights one arm of the modified Mach-Zehnder interferometer (MZIM), which comprises two mirrors. (b) Singles and coincidence interferograms for the MZI experiment. (c) Singles and coincidence interferograms for the MZIM experiment. The coincidence interferograms are similar while the singles interferograms are distinctly different. The insets show data in the vicinity of $\tau = 0$ for each of the four plots; coincidence interferograms oscillate at the pump period, with a frequency twice that of the singles interferograms.

The singles and coincidence rates are presented in Figs. 2(b) and 2(c) for the MZI and MZIM configurations, respectively. The MZI intensity interferogram exhibits nearly 100% visibility ($V_1 = 1$) and has a sinc-like form consistent with a 10-nm bandpass filter of approximately square spectral pass band. The fast oscillation occurs at the down-converted photon frequency $\frac{\omega_p}{2}$, as expected (see inset). The corresponding coincidence interferogram exhibits fast oscillation at the pump period (see its inset) together with an HOM dip. The MZIM coincidence interferogram is nearly identical, but the intensity interferogram is essentially flat, indicating the absence of second-order interference.

Our experimental results therefore reveal that the coincidence measurements of photons at the two output ports yield essentially identical outcomes for both interferometers: high-visibility two-photon interference ($V_{12} = 1$). Yet the singles measurements yield opposite out-

comes: the MZI reveals high-visibility one-photon interference ($V_1 = 1$, in disagreement with the rule-of-thumb), whereas the MZIM reveals the absence of one-photon interference ($V_1 \approx 0$, in agreement with the rule-of-thumb). Unlike the experiments carried out by Walborn et al. [7], the spatial distribution of the source was not modified in going from one experiment to the other.

Let us consider the ways in which photon coincidences at the two output ports of the interferometer may occur. From a simplified viewpoint, there are two distinct possibilities that lead to qualitatively different temporal interference features. In the first of these, each photon emerges from a different port of the first beam splitter. When these photons are brought back at the second beam splitter, after a delay τ in one of the arms, an HOM dip is observed in the coincidence rate $G^{(2)}(\tau)$. In the second possibility, the two photons emerge together from either output port of the first beam splitter. If the frequencies of the two photons, signal and idler, are anti-correlated (which is the case for SPDC with a monochromatic pump, so that $\omega_s = \frac{\omega_p}{2} + \Omega$ and $\omega_i = \frac{\omega_p}{2} - \Omega$, where $\frac{\omega_p}{2}$ is half the pump frequency and Ω is a deviation therefrom), then a delay τ will then lead to a fixed phase difference $\exp\{-i(\frac{\omega_p}{2} + \Omega)\tau\} \exp\{-i(\frac{\omega_p}{2} - \Omega)\tau\} = \exp\{-i\omega_p\tau\}$ between the two paths. In this case, $G^{(2)}(\tau)$ will be a sinusoid at the pump period [12]. These two possibilities coexist in the experimental arrangement shown in Figs. 1 and 2(a), resulting in a coincidence interferogram that combines an HOM dip and a sinusoid at the pump period. Indeed, this is exactly what is observed.

For the singles (intensity) rate at one output port, we expect the usual MZI interferogram, proportional to the second-order temporal coherence function of the optical field. The temporal width of this interferogram should be inversely proportional to the bandwidth of the optical field, as determined by either the source or the detector filter, whichever is narrower. This is, in fact, true for the MZI but, remarkably, it turns out *not* to be true for the MZIM. Rather, the loss of second-order *temporal* interference follows from the *spatial coherence* properties of the source, as we demonstrate below. This surprising result can be understood when the full quantum state, including the spatial distribution of the photons, is taken into consideration [21].

3. Theoretical model

We present a theoretical model that accounts for these results quantitatively. We start by considering a two-photon state that represents both the spectral *and* spatial characteristics of photons, of the form

$$|\Psi\rangle = \int \int dx dx' \int \int d\Omega d\Omega' \phi(x, x') \psi(\Omega, \Omega') |1_{x, \frac{\omega_p}{2} + \Omega}, 1_{x', \frac{\omega_p}{2} + \Omega'}\rangle, \quad (1)$$

with the normalizations $\int \int dx dx' |\phi(x, x')|^2 = 1$ and $\int \int d\Omega d\Omega' |\psi(\Omega, \Omega')|^2 = 1$. Here x and x' are spatial parameters for the signal and idler photons in one dimension (the second dimension y is not taken into consideration without loss of generality); and Ω and Ω' are deviations in frequency from the central frequency $\frac{\omega_p}{2}$. It is essential to note that the two-photon state is assumed to be separable in the spatial-spectral degrees-of-freedom. Thus, while the two photons may be entangled in each of these degrees-of-freedom separately [22], there is no correlation between them. For a monochromatic pump with large transverse spatial dimension (pump width larger than the geometric mean of the pump wavelength and nonlinear-crystal thickness [23]), the entangled state is correlated spatially $\phi(x, x') = \phi(x)\delta(x - x')$ and anti-correlated spectrally $\psi(\Omega, \Omega') = \psi(\Omega)\delta(\Omega + \Omega')$. In this formulation, the function $\psi(\Omega)$ is a baseband function centered at frequency $\Omega = 0$, and $\phi(x)$ is the transverse spatial distribution of the pump [16]. The reduced one-photon state obtained from Eq. (1) is, in general, mixed, and described by the

density operator

$$\rho = \int \int dx dx' \int \int d\Omega d\Omega' \rho_x(x, x') \rho_\Omega(\Omega, \Omega') |1_{x, \frac{\omega_p}{2} + \Omega}\rangle \langle 1_{x', \frac{\omega_p}{2} + \Omega'}|, \quad (2)$$

in which the spatial and spectral degrees-of-freedom remain separable. For a monochromatic pump with large spatial dimension, the state is characterized by $\rho_x(x, x') = |\phi(x)|^2 \delta(x - x')$ and $\rho_\Omega(\Omega, \Omega') = |\psi(\Omega)|^2 \delta(\Omega - \Omega')$.

Next consider the transformation to the state brought about by the MZI and the MZIM. The MZI is characterized by two arms having the same the number of reflections, imparted by mirrors or beam splitters. It can be shown that the MZI conserves the separability of the spatial and spectral degrees-of-freedom of the state of the input optical field, such as the two-photon state set forth in Eq. (1) or the one-photon state provided in Eq. (2). This can be shown by calculating the fourth-order interference at the output, $G^{(2)}(x_1, x_2; \tau)$. For the MZI, this fourth-order coherence function is separable in the spatial and spectral degrees-of-freedom: $G^{(2)}(x_1, x_2; \tau) = G_x^{(2)}(x_1, x_2) G_t^{(2)}(\tau)$. Since the detectors do not register the positions of the photons, but instead integrate over the full transverse domain, the quantity that is measured is $\int \int dx_1 dx_2 G^{(2)}(x_1, x_2; \tau)$, which in this case is simply $G_t^{(2)}(\tau)$. Assuming a monochromatic pump of large spatial extent, we then have

$$G^{(2)}(\tau) = 1 - \frac{1}{2} \cos \omega_p \tau - \frac{1}{2} \int d\Omega |\psi(\Omega)|^2 \cos 2\Omega \tau, \quad (3)$$

where we have assumed, for simplicity, that the spectral density $|\psi(\Omega)|^2$ is an even function. The first term is a constant background, the second is a sinusoid at the pump frequency, and the third is the HOM dip.

The MZI also maintains the separability of the spatial and spectral degrees-of-freedom of the one-photon state provided in Eq. (2). The intensity at the output port thus separates, $G^{(1)}(x_1, x_1; \tau) = I(x_1, \tau) = I_x(x_1) I_t(\tau)$, and the measured intensity as the delay is swept is simply $\int dx_1 I(x_1, \tau) = I_t(\tau)$. This is given by

$$I_t(\tau) = 1 - \cos \frac{\omega_p}{2} \tau \int d\Omega |\psi(\Omega)|^2 \cos \Omega \tau, \quad (4)$$

which is the usual MZI interferogram. It is independent of the spatial distribution and spatial coherence of the input field.

The consequences of removing a mirror from the MZI, which results in an MZIM, are profound. The interferometer no longer preserves the separability of the spatial and spectral degrees-of-freedom of the input state of the field. When the number of mirrors in the two arms of the MZI are not balanced, two copies of the input field reach the detector, differing by a spatial inversion (in one spatial dimension). Unless the field is an eigenfunction of the spatial inversion process [such as even and odd functions $f(-x) = \pm f(x)$], the two copies become distinguishable and do not interfere.

The fourth-order coherence function $G^{(2)}(x_1, x_2; \tau)$, nevertheless, remains the same. Consider the case when the two photons emerge together from the same port of the first beam splitter in the interferometer (the case responsible for the sinusoid at the pump frequency). The spatial probability amplitude when the two photons travel through the arm without the spatial flipper is $\phi(x, x')$, while that in the spatial-flipper arm is $\phi(-x, -x') = \phi(-x) \delta(x - x')$. If the pump transverse spatial distribution is even $\phi(-x) = \phi(x)$, which is the case in our experiment, we have $\phi(-x, -x') = \phi(x, x')$, and the MZIM sinusoid will be identical to that of the MZI. Note that there would result a shift of π , but no change in amplitude, if the pump has an odd spatial distribution $\phi(-x) = -\phi(x)$, and there would be a reduction in amplitude if the pump has

an arbitrary spatial distribution (neither even nor odd). Consider now the case when the two photons emerge from different ports of the first beam splitter (the case responsible for the HOM dip). The two spatial probability amplitudes interfering at the second beam splitter are $\phi(x, -x') = \phi(x)\delta(x+x')$ and $\phi(-x, x') = \phi(-x)\delta(x+x')$. One again, if the pump has an even spatial distribution, the resulting HOM dip is identical to the MZI case. As a result, the fourth-order coherence function is identical for the MZI and MZIM as long as the pump has an even spatial distribution, which is the case in our experiment.

Now consider the second-order coherence function $I(x_1, \tau)$, which differs from that in Eq. (4):

$$I_t(\tau) = 1 - |\alpha| \cos\left(\frac{\omega_p}{2}\tau - \varphi\right) \int d\Omega |\psi(\Omega)|^2 \cos\Omega\tau, \quad (5)$$

where

$$\alpha = |\alpha| e^{i\varphi} = \int dx \rho_x(-x, x). \quad (6)$$

The visibility of the temporal interferogram is thus found to be weighted by a factor α that is a functional of the spatial coherence of the source of the form $\int dx \rho_x(x, -x)$. A field that is spatially incoherent, as in our experiments, $\rho_x(x, x') = |\phi(x)|^2 \delta(x-x')$ results in $\alpha = 0$, thus extinguishing the temporal interference. In other words, since the one-photon field is *spatially* incoherent, the field and its spatially flipped version are mutually incoherent, resulting in the loss of second-order *temporal* interference.

4. Conclusion

In conclusion, we reported two similar experiments that share identical fourth-order interference patterns, but whose second-order interference behaviors are dramatically different. We explain our results in terms of the spatial coherence properties of SPDC, specifically that the two photons possess full spatial coherence when considered jointly, but retain no spatial coherence when considered individually. We remark that the MZIM used to observe this effect may also be used for the measurement of arbitrary optical fields, and thus offers us an important new tool for exploring spatial coherence.

Acknowledgments

This work was supported by a U. S. Army Research Office (ARO) Multidisciplinary University Research Initiative (MURI) Grant and by the Center for Subsurface Sensing and Imaging Systems (CenSSIS), an NSF Engineering Research Center. A. F. A. acknowledges the generous support and encouragement of Y. Fink and J. D. Joannopoulos.